Construction and characterization of a manganese-binding site in cytochrome c peroxidase: towards a novel manganese peroxidase

Bryan KS Yeung*, Xiaotang Wang*, Jeffrey A Sigman, Peter A Petillo and Yi Lu

Background: Manganese-binding sites are found in several heme peroxidases, namely manganese peroxidase (MnP), chloroperoxidase, and the cationic isozyme of peanut peroxidase. The Mn-binding site in MnP is of particular interest. Oxidation of Mn(II) to Mn(III) is a key step in the biodegradation of lignin, a complex phenylpropanoid polymer, as well as of many aromatic pollutants. Cytochrome c peroxidase (CcP), which is structurally homologous to MnP despite a poor sequence homology, does not bind manganese. Thus, engineering a Mn-binding site into CcP will allow us to elucidate principles behind designing metal-binding sites in proteins, to understand the structure and function of this class of Mn-binding centers, and to prepare novel enzymes that can degrade both lignin and other xenobiotic compounds.

Results: Based on a comparison of the crystal structures of CcP and MnP, a site-directed triple mutant (Gly41→Glu, Val45→Glu, His181→Asp) of residues near the putative Mn-binding site in CcP was prepared and purified to homogeneity. Titrating $MnSO_4$ into freshly prepared mutant CcP resulted in electronic absorption spectral changes similar to those observed in MnP. The calculated apparent dissociation constant and the stoichiometry of Mn-binding of CcP were also similar to MnP. Titration with $MnSO_4$ resulted in the disappearance of specific paramagnetically shifted nuclear magnetic resonance spectroscopy signals assigned to residues close to the putative Mn-binding site in the mutant CcP. None of the spectral features were observed in wild-type CcP. In addition, the triple mutant was capable of oxidizing Mn(II) at least five times more efficiently than the native CcP.

Conclusions: A Mn-binding site has been created in CcP and based on our spectroscopic studies the designed Mn-binding site is similar to the Mn-binding site in MnP. The results provide a basis for understanding the structure and function of the Mn-binding site and its role in different heme peroxidases.

Address: Department of Chemistry, University of Illinois at Urbana-Champaign, Urbana, IL 61801, USA.

*Indicates an equal contribution to this work

Correspondence: Yi Lu
E-mail: yi-lu@uiuc.edu

Key words: bioinorganic chemistry, metalloprotein, paramagnetic NMR, protein engineering, site-directed mutagenesis

Received: **11 October 1996**
Revisions requested: **25 October 1996**
Revisions received: **10 February 1997**
Accepted: **4 March 1997**

Electronic identifier: **1074-5521-004-00215**

Chemistry & Biology March 1997, 4:215–221

Introduction

Metal ions are an important class of cofactors in biology. They contribute to biodiversity by fine-tuning the reactivity of biomolecules through their different coordination environments, such as preferred oxidation states, geometry and ligands. Understanding how metal-binding sites are constructed in biomolecules has been the focus of recent studies [1,2]. The principles that govern the design and properties of metal-binding sites are not fully understood, however.

Manganese peroxidase (MnP) is an extracellular heme peroxidase from the white-rot fungus *Phanerochaete chrysosporium* [3] which can degrade both lignin [4], a complex phenylpropanoid polymer, and many xenobiotic compounds such as polychlorinated biphenyls [5,6]. Controlled degradation of lignin could provide renewable energy sources because lignin, the second most abundant renewable material on earth, could be converted into chemicals and fuels. The ability to degrade organic wastes would also allow applications in bioremediation efforts [7].

MnP binds two Ca(II), one Mn(II) and a heme Fe(III) [8]. The Ca(II) sites provide structural support while Mn(II) and the heme Fe(III) are responsible for catalysis. The Mn-binding site has been the focus of recent studies [9,10], and the results have contributed greatly to our understanding of the structure and function of the Mn-binding site in MnP. It is now known that Mn(II) binds to two glutamates, one aspartate, one heme propionate and two water molecules in an octahedral geometry. The enzyme oxidizes Mn(II) to Mn(III) via a hydrogen peroxide

Figure 1

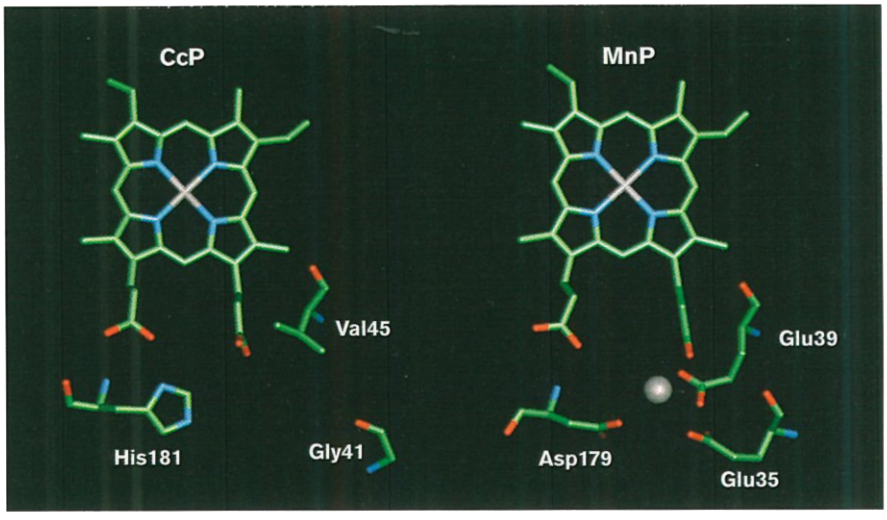

A comparison of the putative Mn-binding site in CcP with the Mn-binding site in MnP. Data taken from [8,15].

(H_2O_2)-generated Fe(IV)=O porphyrin π cation radical which is a key step in the catalytic cycle [3,11]. The enzyme-generated Mn(III) is subsequently used to oxidize organic substrates.

Similar Mn-binding sites have been found in other heme peroxidases, such as chloroperoxidase [12] and the main cationic isozyme of peanut peroxidase [13]. In an effort to understand the construction of the Mn-binding site in heme peroxidase and to elucidate the structural and functional properties, we decided to design and engineer a similar Mn-binding site in cytochrome *c* peroxidase (CcP). CcP served as an ideal template in which to create and study a Mn-binding site because, despite their poor sequence homology, CcP and MnP have comparable structural homology in both their overall fold and their heme active site [8]. In addition, CcP has been extensively characterized by various spectroscopic techniques [14], and its crystal structure has been refined to 1.7Å [15]. Moreover, a recombinant protein expression system has been optimized to produce the CcP proteins in high yield [16–18], and these proteins are amenable to crystallographic characterization [19].

A comparison of the crystal structure of MnP and CcP defined the target for the putative Mn-binding site in CcP [8] (Fig. 1). In MnP, the Mn(II) ion is hexacoordinated to the carboxylate oxygens of Glu35, Glu39, Asp179, a heme propionate oxygen, and two water molecules. One of these water molecules forms a hydrogen bond to the second heme propionate and results in a nearly octahedral geometry typical of Mn(II) complexes. The corresponding site in CcP consists of Gly41, Val45 and His181. In addition, a heme propionate oxygen is available for coordination. We therefore engineered a triple mutant Gly41→Glu, Val45→Glu, His181→Asp in CcP (MnCcP) by site-directed mutagenesis. Spectroscopic characterization by electronic absorption (UV-vis) and paramagnetic nuclear magnetic resonance (NMR) spectroscopy showed that a Mn-binding site that closely mimics the Mn-binding site in MnP had been created in CcP.

Results and discussion

Electronic absorption spectroscopy

Addition of $MnSO_4$ to MnCcP in 100 mM phosphate buffer (pH 6.0) resulted in difference spectra that exhibit maxima at 407 nm and minima at 427 nm (Fig. 2). These spectra are similar to those generated by native MnP [11] and are characteristic of Mn(II) binding near the heme periphery. Following the same procedure used by Wariishi *et al.* [11], the apparent dissociation constant (K_D) and the Mn(II)-binding stoichiometry were estimated using Equations 1 and 2, respectively (see Materials and methods section and Fig. 2). The measured K_D (125.5 μM) in 100 mM phosphate buffer, pH 6.0, was weaker than that of MnP in water (K_D = 9.6 μM) and comparable with that of MnP in buffers containing chelators (K_D = 45.5–153 μM) [11]. The estimated Hill coefficient (0.99) was also similar to that obtained for MnP (0.98–1.04) [11]. Addition of up to 100 equivalents of $MnSO_4$ to wild-type CcP (WTCcP) produced no observable spectral changes under identical experimental conditions (data not shown). These results suggest that a Mn-binding site is created near the heme of CcP and close to the site of the triple mutation.

Electron paramagnetic resonance spectroscopy

The electron paramagnetic resonance (EPR) spectra of wild-type CcP and MnCcP are shown in Figure 3. As reported in the literature, the wild-type CcP displayed a

Figure 2

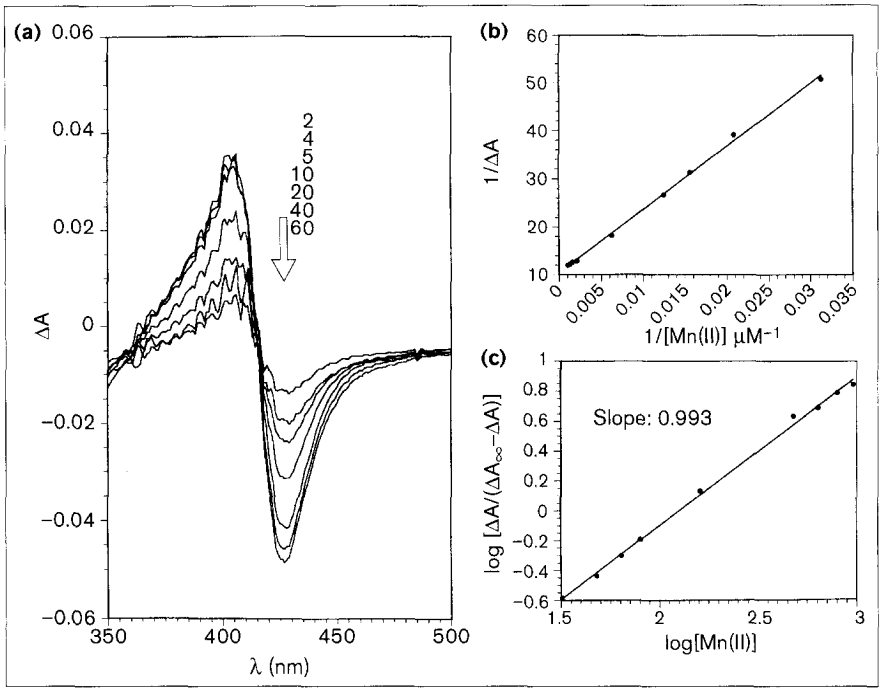

Mn(II) binding to the engineered CcP (MnCcP) in 100 mM phosphate buffer (pH 6.0). **(a)** Difference spectra recorded after the addition of Mn^{2+} to MnCcP. The numbers represent the increasing equivalents of Mn^{2+} added. **(b)** The double reciprocal plot of ΔA versus [Mn(II)], the concentration of Mn(II), yielded the apparent dissociation constant (K_D) and ΔA_∞ from the slope and y-intercept. **(c)** The Hill plot.

predominantly rhombic high-spin signal with $g_z = 1.97$, $g_y = 5.30$ and $g_x = 6.40$ (Fig. 3a) [14,20]. On the other hand, MnCcP displayed an axial high-spin signal with $g_\perp = 5.84$ and $g_\parallel = 2.01$ (Fig. 3b), which are similar to the values for MnP ($g_\perp = 5.79$ and $g_\parallel = 2.00$) [21]. Also, as in MnP [21], no Mn(II) signal (a sextet at g~2) was observed when 10 equivalents of Mn^{2+} ions were added to MnCcP and the proteins were eluted through a Sephadex G25 column to rid the protein of free Mn^{2+} ions. The absence of the Mn(II) EPR signal is not surprising because the Mn-binding affinity of MnCcP ($K_D = 125.5\,\mu M$) is not strong enough to allow the protein to bind Mn(II) after elution from the Sephadex G25 column. This conclusion is supported by inductively coupled plasma emission spectroscopy which shows that MnCcP contains one equivalent of iron, and no manganese or zinc. Thus, it is necessary to design a site with high enough affinity to bind and oxidize Mn(II), but it is equally important to tune the binding affinity so that the Mn(III) can diffuse away to carry out oxidative degradation.

Paramagnetic NMR

The application of paramagnetic NMR spectroscopy to the study of heme peroxidases has now been well established [22]. Considerable insight into the molecular structure and reaction mechanisms can be obtained by correlating the NMR spectral changes induced by factors such as mutation, ligand/substrate binding, and pH, and by examining the consequences associated with such changes [23–25]. To elucidate further the Mn(II) binding in MnCcP, comparative NMR studies were carried out on WTCcP and MnCcP in their cyanide-bound, low-spin forms. Cyanide derivatives are commonly used in

Figure 3

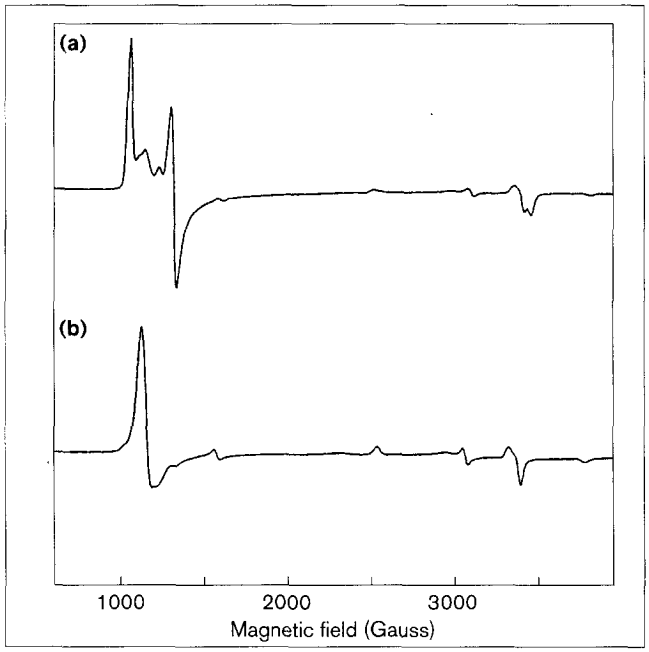

X-band EPR spectra. **(a)** Wild-type CcP (WTCcP) and **(b)** engineered CcP (MnCcP) at 4K. Spectra were obtained on 0.5 mM samples in 100 mM potassium phosphate, pH 6.0 and 50% glycerol.

Figure 4

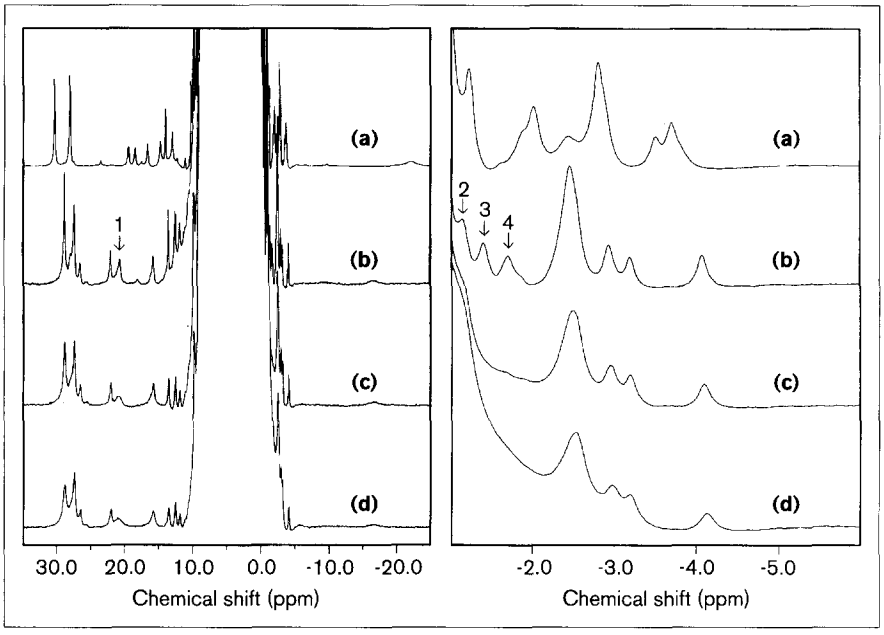

Paramagnetic ^{1}H NMR spectra of cyanide-bound WTCcP and MnCcP. The entire range is shown on the left and an expanded range of −1.0 ppm to −6.0 ppm is shown on the right. **(a)** WTCcP, addition of up to six equivalents of $MnSO_4$ did not produce detectable spectral changes (data not shown). **(b)** MnCcP without $MnSO_4$. Peak 1, the heme 7-propionate α proton; peak 2, Arg48; and peaks 1 and 3, the heme 7-propionate β protons. **(c)** MnCcP with 0.4 equivalents of $MnSO_4$. **(d)** MnCcP with one equivalent of $MnSO_4$. Spectra of WTCcP (0.35 mM) and MnCcP (1.1 mM) were obtained in 80% D_2O solutions (100 mM phosphate) at pH 6.0. Paramagnetically shifted signals assigned to residues near the Mn-binding site (as labeled by the arrows) broaden and disappear upon addition of $MnSO_4$ in MnCcP but not WTCcP.

paramagnetic studies of heme proteins because they give sharper lines and increased signal resolution in the proton NMR spectra than in the native high-spin forms and thus yield more information about the electronic, magnetic and molecular structural properties of the heme pocket [26]. The increased resolution of heme protein cyanide derivatives originate from the relatively large dipolar shifts dictated by large magnetic anisotropy and longer nuclear relaxation times. The dipolar shifts are due to the fast electronic relaxation rate of the low-spin ferric iron [25,27].

The ^{1}H NMR spectra of the cyanide adducts of both WTCcP and MnCcP are shown in Figure 4. The spectrum of WTCcP (Fig. 4a) displays at least two forms of the enzyme under the experimental conditions employed in this study. This heterogeneity has been previously observed and is the result of sample history and the solvent conditions used for collecting the spectrum [28]. Although the spectrum of MnCcP (Fig. 4b) showed several differences from that of the wild-type protein in the hyperfine shifted resonances, the overall spectral pattern is clearly comparable. Further evidence of the spectral similarity between MnCcP and WTCcP has been obtained from one-dimensional and two-dimensional nuclear Overhauser enhancement (NOE) measurements (X.W. and Y.L., unpublished observations).

More importantly, the effects of Mn^{2+} ions on the paramagnetically shifted signals in WTCcP and MnCcP are clearly different. Addition of Mn^{2+} to the MnCcP (Figs 4c,d) significantly broadens signals attributable to those close to the Mn-binding site. In particular, the resonances from the heme 7-propionate α proton (Fig. 4b, peak 1) and β protons (Fig. 4b, peaks 3 and 4) and Arg48 (Fig. 4b, peak 2) are affected most dramatically (these NMR signals have previously been assigned [25,28] and we confirmed the assignment in MnCcP by NOE experiments). The extent of signal broadening is clearly dependent on the Mn^{2+}:protein ratio, and complete broadening was achieved with about one equivalent of Mn^{2+} ions. Similar results have been obtained for manganese peroxidase and were attributed to the presence of a single, high-affinity Mn(II) binding site near the heme periphery [24]. In contrast to MnCcP, no effects were observed when Mn^{2+} was added to WTCcP (Fig. 4a) under identical experimental conditions.

Kinetic studies

Kinetic studies were carried out to investigate the effects of the engineered Mn-binding site on the activity of MnCcP. The electronic absorption spectrum of ferric MnCcP (shown in Fig. 5a, solid line) is similar to that of WTCcP with R_z=1.26. Upon addition of one equivalent of H_2O_2, the ferric MnCcP spectrum was converted into a characteristic spectrum of compound I (heme Fe(IV)=O and tryptophan radical) (see Fig. 5a, dashed line), as seen for WTCcP [16]. Pseudo first-order rate constants of compound I formation were measured using Applied Photophysics' stopped-flow apparatus (see the Materials and methods section). The second-order rate constant was estimated from the slope of the best-fit plot of the pseudo first-order rate constants against the concentration of H_2O_2 (Fig. 5b). The value of the second-order rate constant

Figure 5

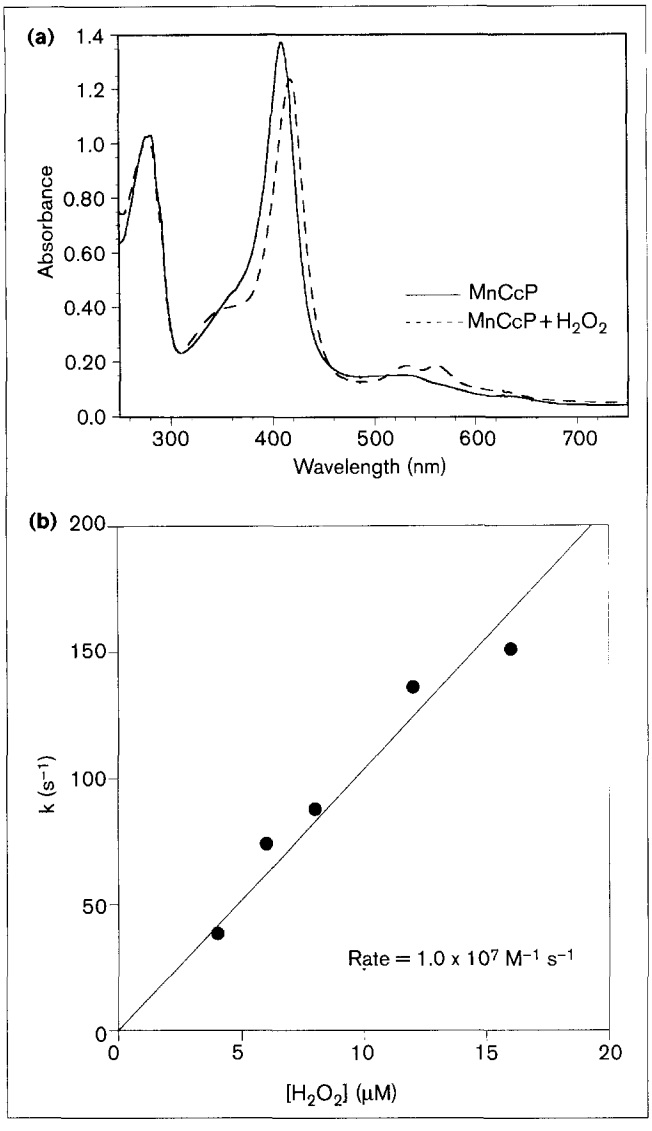

Kinetics of the engineered Mn-binding site. **(a)** Electronic absorption spectra of MnCcP. Solid line, ferric MnCcP (14 μM) in 100 mM potassium phosphate, pH 6.0; dashed line, after addition of one equivalent of H_2O_2. **(b)** Plot of pseudo first-order rate constants versus H_2O_2 concentration (see the Materials and methods section for details). The slope of the best-fit line is the estimated second-order rate constant.

$(1.0\times10^7 M^{-1} s^{-1})$ is comparable to that of WTCcP $(3.0–4.7\times10^7 M^{-1} s^{-1})$ published elsewhere [16–18,29]. These results indicate that the engineered Mn-binding site has no significant effect on the formation of compound I.

In contrast, the ability of MnCcP to oxidize Mn(II) in the presence of H_2O_2 was increased by at least fivefold over that of WTCcP, as monitored by the increase of absorption at 270 nm due to the formation of Mn(III)-malonate (Fig. 6). This result strongly supports the importance of the Mn-binding site in the Mn(II) oxidation activity.

Figure 6

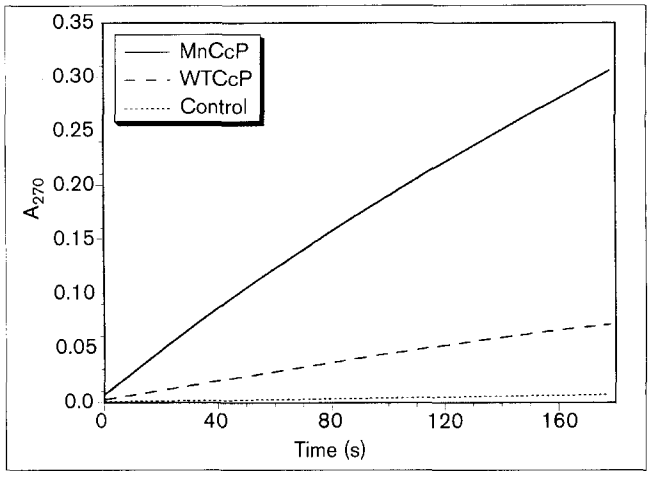

Kinetics of Mn(II) oxidation. The rate of Mn(II)-malonate formation was monitored at 270 nm. Solid line, MnCcP; dashed line, WTCcP; dotted line, no enzyme (control). 20 μg ml^{-1} of enzyme and 6 mM of $MnSO_4$ in 50 mM sodium malonate, pH 6.0 were used. The reaction was initiated by the addition of 1.0 mM H_2O_2.

Even though the Mn(II) oxidation activity of MnCcP was increased over that of WTCcP, the unit activity (0.5 μmol min^{-1} mg^{-1} at pH 6.0) was still far below that of native MnP (377 μmol min^{-1} mg^{-1} at pH 4.5) [30]. Factors contributing to the low activity of MnCcP include, different pH optima, the lower reduction potential of compound I [31] and the formation of a ferryl tryptophan radical rather than the ferryl porphyrin π cation radical [32]. Therefore, based on the structural comparison of WTCcP, MnCcP and MnP, further structural changes are necessary to change the heme iron environment from that in CcP to that in MnP. The combined approach of structural comparison and site-directed mutagenesis will offer insights into the structure and function of MnP and could result in new artificial enzymes that are capable of biodegrading lignin and xenobiotic compounds.

Significance

Metal ions are important in biology and are intrinsically involved in protein structure and catalysis. Understanding how metal-binding sites are constructed and used in biomolecules has been the focus of recent studies. Of particular interest is the manganese-binding site in the heme peroxidase manganese peroxidase (MnP), the functions of which include the biodegradation of lignin and many xenobiotic compounds.

By engineering a Mn-binding site in cytochrome *c* peroxidase (CcP) that closely resembles that of MnP, we have shown that the Mn-binding site may be a common structural motif in all heme peroxidases, despite poor amino acid sequence homology. The results provide a basis for understanding the structure and function of

the Mn-binding site and its role in different heme peroxidases. It opens a new avenue for engineering novel enzymes that are effective in bioremediation and other biotechnological applications.

Materials and methods

Materials

Taq polymerase and restriction endonucleases used in all experiments were purchased from Gibco-BRL (Gaithersburg, MD). Oligonucleotide primers were obtained from the Genetic Engineering Facility at the University of Illinois, USA. The DNA sequencing and mass spectral measurements were carried out at the University of Illinois Biotechnology Center, USA. Chromatographic media was purchased from Pharmacia Biotech (Piscataway, NJ, USA) and PerSeptive Biosystems (Cambridge, MA, USA). H_2O_2 solution was prepared from 30% H_2O_2 solution from Fisher Scientific (Pittsburgh, PA, USA), and its concentration was determined either by its extinction coefficient of 39.4 M^{-1} cm^{-1} at 240 nm [33] or by standardization with $KMnO_4$ [34].

Construction, expression and purification of the site-directed mutant of CcP

The CcP (MI) gene containing the Met–Ile codon was cloned into a pET-17b vector (Novagen, Madison, WI, USA). The expressed protein with Met–Ile at the amino terminus is identical to the native CcP in structural and functional properties, and is thus called WTCcP in this paper. Oligonucleotide site-directed mutagenesis was carried out using a polymerase chain reaction method [35]. A total of two oligonucleotide primers were designed to carry out three point mutations. The first 39-mer, 5′CTT ATG GGT GCT CAC GCT CTG GGC AAG ACC GAC TTG AAG3′, introduced the His181→Asp as well as removing one *Ban*II restriction site. The second 33-mer, 5′GAC AAC TAT ATA GAA TAT GGG CCG GAA TTA GTC CGT3′, introduced Gly41→Glu and Val45→Glu mutations and removed another *Ban*II site. Eliminating two of the three *Ban*II restriction sites in the mutant construct allowed us to monitor whether or not the mutant primers were being incorporated. The sequence of the mutant DNA was confirmed further by DNA sequencing using the dideoxy termination method [36].

The plasmid pET-17b containing Gly41→Glu Val45→Glu and His181→Asp mutations (called MnCcP in this paper) was transformed into BL21(DE3), expressed by induction with isopropyl-β-D-galactopyraniside (IPTG), and purified as described [16–18] with the following modifications. No gel filtration chromatography was carried out. Instead, following heme incorporation the protein was subjected to high performance liquid chromatography (HPLC) purification using a BioCAD Sprint Chromatography system (PerSeptive Biosystems) and Poros HQ 20 anionic exchange media (PerSeptive Biosystems) packed in a Waters AP-1 column (10×60 mm). This purification step generates homogeneous MnCcP and allowed us to skip the final recrystallization steps. The concentration of MnCcP was calculated from a molar absorption coefficient of $\varepsilon_{411} = 93\ mM^{-1}\ cm^{-1}$, estimated from the pyridine hemochromogen method [37,38]. The purified protein was flash frozen and stored at −80°C until use. The purity and identity of MnCcP were also confirmed by amino acid analysis and molecular weight measurement of the apoprotein using a VG Quattro mass spectrometer equipped with an electrospray ionization source.

UV-vis titrations

Titration experiments were performed on an Hewlett-Packard 8453 diode-array spectrophotometer. MnCcP was dialyzed against 100 mM KH_2PO_4, pH 6.0 and 10 mM EDTA twice overnight, followed by several dialyses against 100 mM KH_2PO_4, pH 6.0 to remove EDTA from the sample. MnCcP (16 μM) was placed in both the sample and reference cuvettes. Under gentle stirring, aliquots of 50 mM $MnSO_4$ solution were added to the sample with 2, 3, 4, 5, 10, 30, 40, 50 and 60 equivalents of Mn^{2+} per enzyme equivalent. At the same time, an equal amount of buffer was added to the reference cuvette to compensate for any dilution effects. Difference spectra were obtained in the range of 250–750 nm. MnCcP bound with Mn(II) in phosphate buffer produced a characteristic difference spectra that exhibited maxima at 407 nm and minima at 427 nm. The apparent dissociation constant (K_D) was calculated from the following expression [11]:

$$\frac{1}{\Delta A} = \frac{K_D}{\Delta A_\infty} \times \frac{1}{[S]} + \frac{1}{\Delta A_\infty} \qquad (1)$$

where ΔA is the difference between maximum and minimum absorption, [S] is the concentration of free Mn^{2+}, which was assumed to be equal to the initial concentration, and ΔA_∞ is the absorbance change for the complete formation of the adduct.

The Mn(II) binding to MnCcP in the vicinity of the heme was estimated from the logarithmic form of the Hill equation [11] shown below:D

$$\log\left[\frac{\Delta A}{\Delta A_\infty - \Delta A}\right] = h\log[S] + \log K_D \qquad (2)$$

where ΔA_∞ and K_D were calculated from Equation 1. A plot of $\log[\Delta A/(\Delta A_\infty - \Delta A)]$ against log[S] gave a straight line.

Electron paramagnetic resonance spectroscopy

All EPR experiments were carried out on a Bruker ESP-300 spectrometer fitted with an Oxford Continuous Flow liquid helium cryostat. EPR spectra were obtained at 4K on 0.5 mM protein samples in 100 mM potassium phosphate buffer, pH 6.0 and 50% glycerol. Mn^{2+} was titrated into both WTCcP and MnCcP samples under gentle stirring at 4°C. Both samples were then passed through Pharmacia PD-10 size exclusion columns to remove adventitiously bound Mn(II). Instrument settings: microwave power=9.46 GHz, modulation amplitude=32.4 G, and microwave power=1.00 mW (WTCcP) and 6.32 mW (MnCcP).

Paramagnetic NMR spectroscopy

NMR samples were prepared by three to four times of isotope exchange in deuterated 100 mM KH_2PO_4, pH 6.0 (uncorrected for any isotope effect). Measurements were carried out on 0.35 mM WTCcP and 1.1 mM MnCcP. The low-spin cyanide adducts of the proteins were prepared by addition of a 10-fold excess of cyanide from a freshly made stock solution of 500 mM KCN to the native high-spin ferric enzyme. Proton NMR spectra were recorded at 25°C on a Bruker AMX-600 FTNMR spectrometer operating at 600.14 MHz. All spectra were obtained by collecting 1000–2000 scans with 16384 data points over a 62.5 kHz bandwidth, and a repetition time of 0.5 s with solvent presaturation during the relaxation delay. The FIDs collected were processed with either UXNMR or Felix using 10–20 Hz line broadening. Chemical shifts values were referenced to the residual HDO signal at 4.76 ppm.

Stopped-flow study

The rate of compound I formation was determined using an Applied Photophysics Ltd SX17.MV stopped-flow spectrometer equipped with a 256 element photodiode array detector. The scan rate of the instrument was set to 2.56 ms scan giving a wavelength resolution of 3.3 nm in a 10 mm path length. All experiments were conducted in 100 mM ionic strength potassium phosphate buffer at pH 6.0. The final protein concentration after mixing was 4 μM with a range of H_2O_2 concentrations from 4.0–16 μM. Compound I formation was followed at 427 nm which is the maximum in the difference spectrum between MnCcP compound I and the resting state enzyme. By fitting the rate of change in absorbance at 427 nm to a double exponential, floating end point function:

$$\Delta A = \Delta A_a \exp(-k_a t) + \Delta A_b \exp(-k_b t) + c \qquad (3)$$

values of the rate constants of compound I formation could be obtained at various H_2O_2 concentrations.

Activity assay

The MnP activities of MnCcP and WTCcP were assayed following the method of Wariishi *et al.* [11] using an HP-8453 spectrophotometer

equipped with the manufacturer's kinetic assay package. All assays were carried out at 25°C with a PolyScience digital circulating water bath temperature controller. The protein samples used for the activity assay were treated the same way as samples used for UV-vis titration experiments. Typically, the aqueous reaction mixture consisted of 0.5–6.0 mM $MnSO_4$, 0.1 mM H_2O_2 and 20 μg protein ml^{-1}. The reaction mixture was buffered at pH 6.0 with 50 mM sodium malonate and the reaction was initiated by the addition of H_2O_2. The progress of the reaction was monitored by the formation of Mn(III)-malonate at 270 nm ($\varepsilon = 11.9\,mM^{-1}\,cm^{-1}$), after 5 s of H_2O_2 addition to allow sufficient equilibrium of the system. The reaction was monitored for a total period of 180 s, and the rate constant was calculated from the first 60 s of the reaction with the V_{max} value derived from the Lineweaver–Burk plot.

Supplementary material available

Supplementary material published with this paper on the internet includes the NOE difference spectrum showing the connectivity between the heme 8-CH_3 and one of the α-CH_2 protons from the 7-propionate in MnCcP.

Acknowledgements

We thank James Kaput and James Erman for the generous gift of the gene encoding CcP, Sung Syn for technical assistance, Robert R Gennis for use of a stopped-flow apparatus, and Harold Goff and John Snyder for use of the NMR facility at the University of Iowa. This research is supported by the National Science Foundation (CAREER award CHE 95-02421) and the Arnold and Mabel Beckman Foundation (Beckman Young Investigator Award).

References

1. Regan, L. (1995). Protein design: novel metal binding sites. *Trends Biochem. Sci.* **20**, 280–285.
2. Kellis, J.T., Jr, Todd, R.J. & Arnold, F.H. (1991). Protein stabilization by engineered metal chelation. *Biotechnology* **9**, 994–995.
3. Gold, M.H., Wariishi, H. & Valli, K. (1989). Extracellular peroxidases involved in lignin degradation by the white rot basidiomycete *Phanerochaete chrysosporium*. In *Biocatalysis in Agricultural Biotechnology*. (Whitaker, J.R. & Sonnet, P.E., eds), pp. 127–140, American Chemical Society, Washington, DC, USA.
4. Gold, M. & Alic, M. (1993). Molecular biology of the lignin-degrading basidiomycete *Phanerochaete chrysosporium*. *Microbiol. Rev.* **57**, 605–622.
5. Bumpus, J.A. & Aust, S.D. (1987). Biodegradation of environmental pollutants by the white rot fungus *Phanerochaete chrysosporium*: involvement of the lignin degrading system. *Bioessays* **6**, 166–170.
6. Eaton, D.C. (1985). Mineralization of polychlorinated biphenyls by *Phanerochaete chrysosporium*: a ligninolytic fungus. *Enzyme Microb. Technol.* **7**, 194–196.
7. Paszczynski, A. & Crawford, R.L. (1995). Potential for bioremediation of xenobiotic compounds by the white-rot fungus *Phanerochaete chrysosporium*. *Biotechnol. Prog.* **11**, 368–379.
8. Sundaramoorthy, M., Kishi, K., Gold, M.H. & Poulos, T.L. (1994). The crystal structure of manganese peroxidase from *Phanerochaete chrysosporium* at 2.06 Å resolution. *J. Biol. Chem.* **269**, 32759–32767.
9. Kuan, I.-C., Johnson, K.A. & Tien, M. (1993). Kinetic analysis of manganese peroxidase. *J. Biol. Chem.* **268**, 20064–20070.
10. Kishi, K., Someren, M.K., Mayfield, M.B., Sun, J., Loehr, T.M. & Gold, M.H. (1996). Characterization of manganese(II) binding site mutants of manganese peroxidase. *Biochemistry* **35**, 8986–8994.
11. Wariishi, H., Valli, K. & Gold, M.H. (1992). Manganese(II) oxidation by manganese peroxidase from the basidiomycete *Phanerochaete chrysosporium*. *J. Biol. Chem.* **267**, 23688–23695.
12. Sundaramoorthy, M., Terner, J. & Poulos, T.L. (1995). The crystal structure of chloroperoxidase: a heme peroxidase-cytochrome P450 functional hybrid. *Structure* **3**, 1367–1377.
13. Rodríguez Marañón, M.J., Hoy, A.R. & Van Huystee, R.B. (1994). Evidence for the presence of Mn(II) in a peanut peroxidase. An EPR study. *Cell. Mol. Biol.* **40**, 871–879.
14. Bosshard, H.R., Anni, H. & Yonetani, T. (1991). Yeast cytochrome c peroxidase. In *Peroxidases in Chemistry and Biology*, II. (Everse, J. & Grisham, M.B., eds) pp. 51–84, CRC Press: Boca Raton, FL, USA.
15. Finzel, B.C., Poulos, T.L. & Kraut, J. (1984). Crystal structure of yeast cytochrome c peroxidase refined at 1.7 Å resolution. *J. Biol. Chem.* **259**, 13027–13036.
16. Fishel, L.A., Villafranca, J.E., Mauro, J.M. & Kraut, J. (1987). Yeast cytochrome c peroxidase: mutagenesis and expression in *Escherichia coli* show trptophan-51 is not the radical site in compound I. *Biochemistry* **26**, 351–360.
17. Choudhury, K., *et al.*, & Poulos, T.L. (1994). Role of the proximal ligand in peroxidase catalysis. *J. Biol. Chem.* **269**, 20239–20249.
18. Goodin, D.B., Davison, M.G., Roe, J.A., Mauk, A.G. & Smith, M. (1991). Amino acid substitutions at tryptophan-51 of cytochrome c peroxidase: effects on coordination, species preference for cytochrome c, and electron transfer. *Biochemistry* **30**, 4953–4962.
19. Poulos, T.L. & Fenna, R.E. (1994). Peroxidases: structure, function, and engineering. In *Metal Ions in Biological Systems: Metalloenzymes Involving Amino Acid Residue and Related Radicals*. (Sigal, H. & Sigal, A., eds), pp. 25–75, Marcel Dekker, NY, USA.
20. Hashimoto, S., Teraoka, J., Inubushi, T., Yonetani, T. & Kitagawa, T. (1986). Resonance Raman study on cytochrome c peroxidase and its intermediate. Presence of the Fe(IV)=O bond in compound ES and heme-linked ionization. *J. Biol. Chem.* **261**, 11110–11118.
21. Mino, Y., Wariishi, H., Blackburn, N.J., Loehr, T.M. & Gold, M.H. (1988). Spectral characterization of manganese peroxidase, an extracellular heme enzyme from the lignin-degrading basidiomycete, *Phanerochaete chrysosporium*. *J. Biol. Chem.* **263**, 7029–7036.
22. Bertini, I., Turano, P. & Vila, A.J. (1993). Nuclear magnetic resonance of paramagnetic metalloproteins. *Chem. Rev.* **93**, 2833–2892.
23. Banci, L., Bertini, I., Bren, K.L., Gray, H.B. & Turano, P. (1995). pH-Dependent equilibria of yeast Met80Ala-iso-1-cytochrome c probed by NMR spectroscopy: a comparison with the wild-type protein. *Chem. Biol.* **2**, 377–383.
24. Banci, L., Bertini, I., Bini, T., Tien, M. & Turano, P. (1993). Binding of horseradish, lignin, and manganese peroxidase to their respective substrates. *Biochemistry* **32**, 5825–5831.
25. Satterlee, J.D., Alam, S.L., Mauro, M.J., Erman, J.E. & Poulos, T.L. (1994). The effect of the Asn82→Asp mutation in yeast cytochrome c peroxidase studied by proton NMR spectroscopy. *Eur. J. Biochem.* **224**, 81–87.
26. Bertini, I. & Luchinat, C. (1986). NMR of Paramagnetic Molecules in Biological Systems. Benjamin-Cummings, Menlo Park, CA, USA.
27. La Mar, G.N. & De Ropp, J.S. (1993). NMR Methodology for Paramagnetic Proteins. In *Biological Magnetic Resonance*. (Berliner, L.J. & Reuben, J., eds), pp. 1–78, Plenum Press, NY, USA.
28. Satterlee, J.D., Erman, J.E., Mauro, M.J. & Kraut, J. (1990). Comparative proton NMR analysis of wild-type cytochrome c peroxidase from yeast, the recombinant enzyme from *Escherichia coli*, and an Asp→Asn235 mutant. *Biochemistry* **29**, 8797–8804.
29. Erman, J.E., Vitello, L.B., Miller, M.A., Shaw, A., Brown, K.A. & Kraut, J. (1993). Histidine 52 is a critical residue for rapid formation of cytochrome c peroxidase compound I. *Biochemistry* **32**, 9798–9806.
30. Mayfield, M.B., Kishi, K., Alic, M. & Gold, M.H. (1994). Homologous expression of recombinant manganese peroxidase in *Phanerochaete chrysosporium*. *Appl. Environ. Microbiol.* **60**, 4303–4309.
31. Mondal, M.S., Fuller, H.A. & Armstrong, F.A. (1996). Direct measurement of the reduction potential of catalytically active cytochrome c peroxidase compound I: voltammetric detection of a reversible, cooperative two-electron transfer reaction. *J. Am. Chem. Soc.* **118**, 263–264.
32. Sivaraja, M., Goodin, D.B., Smith, M. & Hoffman, B.M. (1989). Identification by ENDOR of Trp191 as the free-radical site in cytochrome c peroxidase compound ES. *Science* **245**, 738–740.
33. Nelson, D.P. & Kiesow, L.A. (1972). Enthalpy of decomposition of hydrogen peroxide by catalase at 25°C. *Anal. Biochem.* **49**, 474–478.
34. Skoog, D.A., West, D.M. & Holler, F.J. (1992). Fundamentals of Analytical Chemistry (6th edn), Saunders College Publishing, Orlando, FL, USA.
35. Reikofski, J. & Tao, B.Y. (1992). Polymerase chain reaction (PCR) techniques for site-directed mutagenesis. *Biotech. Adv.* **10**, 535–547.
36. Sanger, F.S., Nicklem, S. & Coulson, A.R. (1977). DNA sequencing with chain-terminating inhibitors. *Proc. Natl. Acad. Sci. USA* **74**, 5463–5467.
37. De Duve, C. (1948). A spectrophotometric method for the simultaneous determination of myoglobin and hemoglobin in extracts of human muscle. *Acta Chem. Scand.* **2**, 264–289.
38. Morrison, M. & Horie, S. (1965). Determination of heme a concentration in cytochrome preparations by hemochromogen method. *Anal. Biochem.* **12**, 77–82.